Caveolin-1β promotes the production of active human microsomal glutathione S-transferase in induced intracellular vesicles in *Spodoptera frugiperda* insect cells

Nahuel Perrot, Delphine Dessaux, Anthony Rignani, Cynthia Gillet, Stéphane Orlowski, Nadège Jamin, Manuel Garrigos, Christine Jaxel

BBA - Biomembranes 1864 (2022) 183922

Contents lists available at ScienceDirect

BBA - Biomembranes

journal homepage: www.elsevier.com/locate/bbamem

Caveolin-1β promotes the production of active human microsomal glutathione S-transferase in induced intracellular vesicles in *Spodoptera frugiperda 21* insect cells

Nahuel Perrot [1,2], Delphine Dessaux [1,3], Anthony Rignani [4], Cynthia Gillet, Stéphane Orlowski [*], Nadège Jamin [*], Manuel Garrigos, Christine Jaxel [*]

Université Paris-Saclay, CEA, CNRS, Institute for Integrative Biology of the Cell (I2BC), 91198 Gif-sur-Yvette, France

ARTICLE INFO

Keywords:
Sf21 insect cells
Heterologous co-expression
Membrane protein
Canine caveolin-1β
Human MGST1
Membrane remodeling

ABSTRACT

The heterologous expression in *Spodoptera frugiperda 21* (*Sf21*) insect cells of the β isoform of canine caveolin-1 (caveolin-1β), using a baculovirus-based vector, resulted in intracellular vesicles enriched in caveolin-1β. We investigated whether these vesicles could act as membrane reservoirs, and promote the production of an active membrane protein (MP) when co-expressed with caveolin-1β. We chose hMGST1 (human microsomal glutathione S-transferase 1) as the co-expressed MP. It belongs to the membrane-associated proteins in eicosanoid and glutathione metabolism (MAPEG) family of integral MPs, and, as a phase II detoxification enzyme, it catalyzes glutathione conjugation of lipophilic drugs present in the lipid membranes. In addition to its pharmaceutical interest, its GST activity can be conveniently measured. The expression of both MPs were followed by Western blots and membrane fractionation on density gradient, and their cell localization by immunolabeling and transmission electron microscopy. We showed that caveolin-1β kept its capacity to induce intracellular vesicles in the host when co-expressed with hMGST1, and that hMGST1 is in part addressed to these vesicles. Remarkably, a fourfold increase in the amount of active hMGST1 was found in the most enriched membrane fraction, along with an increase of its specific activity by 60% when it was co-expressed with caveolin-1β. Thus, heterologously expressed caveolin-1β was able to induce cytoplasmic vesicles in which a co-expressed exogenous MP is diverted and sequestered, providing a favorable environment for this cargo.

1. Introduction

Membrane proteins (MPs) play crucial roles in a wide variety of cellular processes, such as signal transduction, cell homeostasis processes and control of membrane lipid compositions. Many diseases are caused by mutations of MPs. The importance of these proteins is also highlighted by the facts that they account for 30% of the human proteome and that more than 50% of drugs target this class of proteins [1]. For a better understanding of their cellular role, a detailed knowledge of their function and structure at a molecular level is required.

Except for few MPs, one of the major obstacles to acquire such knowledge is related to their constitutively low abundance in native cells. But, when investigating the structure and the function of MPs, it is necessary to combine both a membrane environment [2] and the possibility to perform site-directed mutagenesis combined with activity tests. Therefore, for such studies, MPs are efficiently produced using overexpression in heterologous cell systems, among which insect cells (*Spodoptera frugiperda*, *Sf9* and *Sf21* cells) [3]. These cells have been the prominent heterologous expression system for the production of eukaryotic MPs, which has allowed to obtain various molecular

* Corresponding authors at: Institut Joliot/SB2SM, I2BC, Bâtiment 528, PC 103, CEA Saclay, 91191 Gif-sur-Yvette cedex, France.
E-mail addresses: nperrot@bidmc.harvard.edu (N. Perrot), dessaux@insa-toulouse.fr (D. Dessaux), stephane.orlowski@i2bc.paris-saclay.fr (S. Orlowski), nadege.jamin@i2bc.paris-saclay.fr (N. Jamin), christine.jaxel@i2bc.paris-saclay.fr (C. Jaxel).
[1] Nahuel Perrot and Delphine Dessaux contributed equally to this work.
[2] Present address: Beth Israël Deaconess Medical Center, Harvard Medical School, Division of Hematology/Oncology, 330 Brookline avenue, Boston, MA 02215, USA.
[3] Present address: Toulouse Biotechnology Institute, Université de Toulouse, CNRS, INRAE, INSA, Toulouse, France.
[4] Present address: 3 ter route de Chevreuse, 91190 Gif sur Yvette, France.

https://doi.org/10.1016/j.bbamem.2022.183922
Received 6 October 2021; Received in revised form 22 March 2022; Accepted 24 March 2022
Available online 30 March 2022

structures over the recent years [4]. As a matter of fact, lipid content, post-translational modifications, and protein folding in insect cells more closely resemble that in mammalian cells than other cost-effective expression systems, such as bacterial and yeast systems. In addition, compared to insect cells, mammalian cells, such as HEK293 cells, generally yield lower quantities of produced recombinant proteins and require larger amounts of plasmid for the transfection process (for reviews, see [4,5]).

In mammalian cells, caveolin-1, an integral membrane protein of 21 kDa, is the main and characteristic membrane protein component of *caveolae* membranes. Caveolin-1 is synthesized as a hairpin-like monotopic membrane protein in the endoplasmic reticulum (ER) [6]. The newly synthesized protein goes through a first stage of oligomerization, which occurs in the ER. Caveolin-1 is then transported from the ER to the Golgi complex. Further integration into the plasma membrane, to form the typical *caveolae* structures, requires the association with specific protein partners, such as cavins (for reviews see [7,8]).

The heterologous overexpression, using baculovirus system, of either isoform α or β of canine caveolin-1 has been reported to induce the production of numerous cytosolic vesicles in *Sf21* insect cells [9]. For this study, a Myc epitope tag was placed at the C-terminus of both caveolin isoforms, followed by a polyhistidine tag [9]. These accumulated vesicles present in the insect cells infected with a recombinant baculovirus were purified by equilibrium sucrose density gradient system [10,11]. After examination by electron microscopy, these membranous vesicles appeared as 50–100 nm structures, and were immunogold labeled with anti-caveolin-1 IgG. Moreover, the authors also demonstrated that a soluble protein, Hα-Ras, supposed to interact with caveolin-1 in mammalian cells, was able to interact with the protein when they were simultaneously both expressed in *Sf21* cells by co-infection with two distinct recombinant baculoviruses [10,11].

More recently, Walser et al. found that the expression, in *E. coli*, of the recombinant caveolin-1, MBP-TEV-Cav-1α (1-178)-His6 [12] led to the formation of intracellular membranous vesicles that were called heterologous *caveolae* (h-*caveolae*). These vesicles, 45–50 nm in diameter, were observed within the bacteria cytoplasm, and specific labeling with anti-MBP antibodies against the recombinant protein was detected.

In addition, using *E. coli* as expression system host, Shin et al., have co-expressed caveolin-1α and two transmembrane SNARE (soluble N-ethylmaleimide-sensitive factor attachment protein receptor) proteins, syntaxin 1a and vesicle-associated membrane protein 2 (VAMP2), to test the possible repercussion of either MP on the formation of h-*caveolae* and whether they are functionally incorporated in these vesicles. Actually, the co-expressed MPs and caveolin-1α were detected by Western blots in intracellular vesicles and, moreover, the VAMP2 protein associated with caveolin-1α vesicles was functionally able to form a SNARE complex by membrane fusion [13]. However, no evidence of a colocalisation of the co-expressed MP and caveolin-1α was shown.

To our knowledge, no attempt has been made to co-express a MP with caveolin-1 in eukaryotic cells such as insect cells. In this context, our objective was to evaluate, in *Sf21* insect cells using baculovirus system, the effect of the co-expression of caveolin-1β on the production of the human microsomal glutathione S-transferase 1 (hMGST1). This MP catalyzes glutathione conjugation of lipophilic substrates present in the lipid membranes [14]. As a matter of fact, even if both rat and human MGST1 have been expressed in COS simian cells and *E. coli*, the human isoform appeared to be less easy to handle [15,16].

Glutathione S-transferase (GST) activity has emerged independently at least four different times throughout evolutionary history, producing four different GST families: cytosolic, microsomal, mitochondrial, and bacterial [17]. The three first subfamilies of enzymes are present in various species. As an example, sequencing the *Tribolium castaneum* genome identified thirty-six putative cytosolic GSTs and five microsomal GSTs [18]. More specifically, in *Sf21* cells, seven MGST homologues have been found (J. Landry, EMBL, personal communication). Glutathione S-transferases are major detoxification enzymes, in particular involved in insecticide resistance. The microsomal enzymes family has been recently included in a new superfamily, termed the MAPEG (membrane-associated proteins in eicosanoid and glutathione metabolism). This superfamily is represented in all life forms, except *archae* [14]. The MAPEG superfamily was defined based on enzymatic activities, structural properties, and sequence similarities [19]. The first MAPEG structure solved, in 2006, was that of rat MGST1 [20], and it does not share structural similarity with the other family members. The microsomal enzymes are shorter than cytosolic ones, by around 150–160 amino acids, and some members of the family have been shown to be trimers [19,21,22]. In humans, three different MGSTs have been described: hMGST1, hMGST2 and hMGST3 [23].

The GSTs play a major role in the detoxification and excretion of xenobiotics [24], including some cytotoxic drugs [14]. In plants and animals, GSTs are the main phase II enzymes in metabolic detoxification processes [25]. As a potent physiological reducing agent, the tripeptide glutathione (GSH: γ-Glu-Cys-Gly) is the most abundant intracellular small molecule thiol, reaching millimolar concentrations in most cell types in higher organisms [26]. The main enzyme chemistry is to catalyze the conjugation of GSH with compounds containing an electrophilic center, to form more soluble, non-toxic derivatives, ready to be excreted or compartmentalized by phase III transporters [27]. The substrates of the MGSTs resemble one another in that they are all electrophilic and hydrophobic, allowing their membrane access to the enzyme active site. In addition, the MGSTs have a special complementary role to play in drug metabolism. Indeed, the cytochrome P-450 system belongs to the phase I cell detoxification process, and produces many of the reactive intermediates of xenobiotic metabolism that can serve as substrates for the MGSTs due to their colocalization in the same membrane [28]. In the case of MGST1, its presence has been detected in the endoplasmic reticulum and other organelles such as mitochondria [29], plasma membranes [30] and peroxysomes [31]. MGSTs also possess a GSH peroxidase activity, allowing it to counter lipid peroxidation and more generally to play a protective role against cellular oxidative stress [32]. In addition to its pharmaceutical interest, MGSTs display an easily-measurable activity, according to its capability to catalyze GSH conjugation to 1-chloro-2,4-dinitrobenzene (CDNB), as determined spectrophotometrically at 340 nm by the method of Habig et al., [33]. These characteristics validate our choice of hMGST1 as a model MP to study its heterologous expression.

In the present study, we asked whether the heterologous overexpression of caveolin-1β may affect the co-expression of a MP, and reciprocally, taking into account the induced remodeling of intracellular membranes. In particular, we checked the hypothesis that the intracellular vesicles produced by the overexpression of caveolin-1β in *Sf21* cells may serve as membrane reservoirs that may promote the production of a functional MP. In that context, hMGST1 was co-expressed with caveolin-1β using baculovirus system. Starting with a co-expression vector, a unique baculovirus was used for the infection of the insect cells. The production of intracellular vesicles and the presence of both proteins was followed by immuno-labeling for transmission electron microscopy and Western blots, and the GST activity of hMGST1 was determined. By distinguishing the two enzymatic pools of the expressed hMGST1 and the endogenous MGSTs from the insect cells, we found that the co-expression of caveolin-1β induces a shift of the density of the membranes expressing hMGST1, and that hMGST1 exhibits an enhanced production in these membrane fractions, with an increased specific enzymatic activity.

2. Materials and methods

2.1. Materials

Biochemical products were from Sigma-Aldrich (Lyon, France) unless specified otherwise. Restriction and modification enzymes, as Calf Intestinal Alkaline Phosphatase (CIP) (M0290) and T4 DNA ligase

(M0202), were purchased from New England Biolabs (Beverly, MA, USA). The Clone JET PCR cloning kit (K1232) was from Thermo Scientific. Quik-Pik Electroelution capsules were from Bioscience. ECL WB detection reagents GE Healthcare were from Dutscher. Antibodies were from: Abcam for antibodies against MGST1 (EPR 7934-ab131059 and EPR 7935-ab129175), Thermofisher Scientific for antibody against MGST1 (MA5-34942), and BD Biosciences for purified mouse anti-caveolin-1 clone 2297 (610407). Secondary antibodies HRP-conjugates were from Biorad for goat anti-rabbit IgG (170-6515) and from Invitrogen for goat anti-mouse IgG1 (PA1-74421). His-probe HRP conjugate and Sf900 II SFM medium were from Thermofisher Scientific.

Products for bacteria cultures were purchased from Difco (Detroit, MI, USA).

Precision protein standards were from Biorad. Immobilon-P membranes PVDF 0.2 μm were from Millipore (Bedford, MA, USA).

Products for immunodetection observable by transmission electronic microscopy were from Aurion: anti-rabbit antibody coupled to 6 nm gold nano-particles, anti-mouse antibody coupled to 6 gold nano-particles, PBS 0.1% (w:v) acetylated bovine serum albumin solution # 900.099 (PBS 0.1% BSAc), blocking solution for goat gold conjugates # 905.002 (blocking solution). Methylamine vanadate (NanoVan) was from Cliniscience.

2.2. Construction of baculovirus

The isoform β of canine caveolin-1 was cloned in a MultiBac plasmid (pKL [34] with a 10-His tag and a TEV site on the N-terminus), and its expression is under the control of a polyhedron (polH) promoter. The hMGST1 was cloned under a p10 promoter in the pKL plasmid, alone or in tandem with the polH-caveolin-1β expression cassette (Fig. S1). Each plasmid was integrated in a Yellow Green Protein (YFP) containing bacmid by transformation in EMBACY *E. coli* strain (a derivative of DH10MultiBac strain). The resulting recombinant bacmids were used to transfect *Sf21* insect cells, giving the V0 virus generation. After amplification, stocks of viruses were titrated by the dilution limit method using YFP as a marker for infected cells and Mac Grady Table.

2.3. Growth of Sf21 insect cells

Proteins production was initiated by infection with baculovirus (Bacmid) at MOI of 5.10^{-3} in three 3 L Erlenmeyers containing 600 mL of culture at 5.10^5 *Sf21* cells per mL and 10 μg mL^{-1} of gentamicin each. The infected cultures were incubated at 27 °C with a 120 rpm agitation during 2 days, time necessary for cell growth and viral infection. The culture contains about 2.10^6 cells per mL, and the infection rate is measured by fluorescence. Indeed, a gene coding for YFP protein is present on the Bacmid as a protein production reporter. Thus, the production of this protein followed on a benchtop cytometer (Guava® easyCyte 6HT) allows additionally a measure of viral infection. During the 3 following days, cells do not grow, and the proteins production increases. Culture (6 × 300 mL) was centrifuged at 500 ×*g* (rotor Beckman JA10) for 4 min at 4 °C. Each pellet containing about 2.10^8 cells was finally conserved at −80 °C.

2.4. Preparation of membrane fractions

In order to preserve GST activity, all the steps were performed in a cold room, at 4 °C, in the presence of 10% (v:v) glycerol and 1 mM GSH, and 1 mM PMSF was added to the solution every hour. The weight of pellets (P) was measured (P ≈ 5 g). Pellets were suspended in a low salt A buffer (10 mM Hepes pH 8.0, 10 mM NaCl, 10% (v:v) glycerol, 1 mM GSH) in a total volume equivalent to 2 P (≈10 mL). PMSF and proteases inhibitors cocktail were added to reach 1 mM and 1 mL for 10 g of cells (final amounts), respectively. After 50 min incubation, gentle cell lysis was performed by Potter-homogenization (cycles of 2 min homogenization and 3 min stop, at 4 °C). Cell lysis was followed by microscopy. After 3 h of Potter-homogenization at 4 °C, this suspension was centrifuged at 1000 ×*g* (rotor Beckman JA14.5) for 20 min at 4 °C to eliminate cell debris and nuclei. The supernatants were then centrifuged at 9500 ×*g* (rotor Beckman TL100.3) for 40 min at 4 °C to pellet mitochondria and lysosomes, allowing the isolation of a pellet (P2) enriched in cell membranes [35]. Pellets were suspended in 4 mL of B buffer (25 mM sodium phosphate pH 7.4, 150 mM NaCl, 10% (v:v) glycerol, 1 mM GSH, 1 mM PMSF) loaded onto a sucrose cushion (1 mL of a 50% (w:w) sucrose in B buffer) and centrifuged at 70,000 ×*g* (rotor Beckman TL100.3) for 1 h at 4 °C. Then a floating crude fraction, called total membranes (TM), was collected at the interface above the cushion. A final step was realized by loading the TM fraction onto a continuous sucrose gradients (28–46% (w:w) in B buffer) followed by an isopycnic centrifugation at 150,000 ×*g* (rotor Beckman SW41) for 24 h at 4 °C, in order to further separate the membrane vesicles fractions (Fig. 1). Collects of 0.5 or 1 mL fractions, as indicated, were performed from the top of the centrifugation tubes. For each fraction, the protein concentration and refractive index (n) were determined (Fig. S2), and fractions were then analyzed for caveolin 1β and hMGST1 contents and hMGST1 activity.

2.5. SDS–PAGE and blotting

For SDS–PAGE, aliquots were mixed with an equal volume of denaturing buffer (100 mM Tris–HCl pH 8.0, 1.4 M β-mercaptoethanol, 4% (w/v) SDS, 5 mM EDTA, 8 M urea, 0.05% (w/v) bromophenol blue). Amounts of proteins of initial samples loaded in each well are indicated in the Figure legends. Rat microsomes were a gift of Marcel Delaforge who prepared them according to [36]. Samples were heated at 100 °C for 2 min [37,38], cooled and then loaded onto a Laemmli-type 14% (w/v) polyacrylamide gel. These gels were used for blotting. Proteins were transferred onto PVDF membrane (Immobilon-P) in cold buffer (27.6 mM Tris, 192 mM glycine, 10% (v/v) methanol). Western blotting was followed either by immunodetection with a monoclonal antibody anti-MGST1 and a secondary antibody anti-rabbit, or by detection with histidine–peroxidase probe for the recognition of histidine tagged proteins, as described by the manufacturer. After the saturation step with 2% (w:v) BSA in PBS-Tween buffer (90 mM K_2HPO_4, 10 mM KH_2PO_4 pH 7.7, 100 mM NaCl, 0.2% (v/v) Tween 20), a 30 min incubation with the first reagent was carried out in the presence of 2% (w:v) BSA. This was

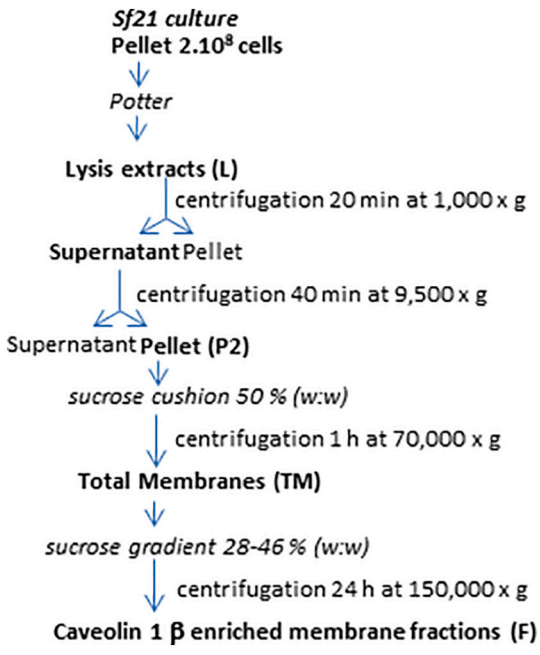

Fig. 1. Procedure for the preparation of membrane fractions from *Sf21* insect cells.

followed by several washes with PBS-Tween buffer before the second 30 min incubation, for immunodetection, with secondary antibodies in the same buffer with 2% (w:v) BSA. After final washes with PBS-Tween buffer, blots were revealed by enhanced chemiluminescence with the ECL kit (GE Healthcare). In the case of anti-MGST1 EPR 7934 immunodetection, the ECL prime was used.

For each gel, molecular mass markers were loaded. For Western blots, the positions of molecular mass markers are indicated relative to their positions on the PVDF membranes.

2.6. Transmission electron microscopy (TEM)

2.6.1. Cells preparation for ultrastructural study

Cells were fixed 1 h30 at room temperature (RT) with 2.5% glutaraldehyde in 0.1 M phosphate buffer (PB) pH 7.4. After washing with buffer, cells were post-fixed 1 h with 1% osmium and 1.5% potassium ferrocyanide. Pellets were then centrifuged in 2% low melting point agarose to facilitate their handling. Samples were progressively dehydrated in graded ethanol series (30-50-70-90-100%), and finally in propylene oxide before the resin embedding. Embedding in epoxy resin (Low Viscosity Premix Kit Medium, Agar Scientific, Oxford instruments) was performed on 3 days (25-50-75-100%). Blocs were polymerized for 24 h at 60 °C.

Ultrathin sections (80 nm) were cut with an ultramicrotome EM UC6 (Leica Microsystems), collected on formvar carbon-coated copper grids, and then stained with 2% uranyl acetate (Merck) and lead citrate before observation.

2.6.2. Immunodetection on insect cells

Cells were transferred for 1 h to fixative (4% paraformaldehyde (PFA) in PB buffer) and rinsed 3 times in buffer. Samples were then incubated 10 min in 50 mM glycine to quench aldehyde, and rinsed 3 times in buffer before final embedding in 12% gelatine (Sigma-Aldrich, G2500). The gelatine blocks (1 mm^3) were infiltrated overnight in 2.63 M sucrose, frozen by plunging into liquid nitrogen (LN_2). Samples were finally stored in LN_2, until sectioning by cryo-ultramicrotomy (EM UC6, Leica Microsystems). For immunolabeling, 70 nm-sections were floated successively 5 min in 0.5% Tween-PBS, 30 min in blocking solution, 10 min in PBS 0.1% BSAc, and incubated overnight at 4 °C in the caveolin-1 or MGST1 (MA5-34942, Thermofisher Scientific) primary antibodies (1:10). The sections were washed several times in PBS 0.1% BSAc, and incubated 30 min at RT with a 1:20 dilution of an anti-mouse secondary antibody conjugated to 6 nm gold particles. Sections were stained with uranyl acetate/methylcellulose mix before TEM imaging.

2.6.3. Immunodetection on isolated membrane vesicles

The sucrose membrane fraction of interest was dialyzed overnight against PBS buffer (10 mM sodium phosphate pH 7.4, 150 mM NaCl) at RT. A volume sample of 600 μL (0.75 mg mL^{-1}) was mixed with 200 μL of PFA 16% (v:v) to fix the protein structure. Then, the sample was loaded on the grid, which was washed with several solutions: PBS buffer, blocking solution, PBS 50 mM glycine solution (adjusted at pH 8.0), PBS buffer and PBS 0.1% BSAc. The grid was incubated 1 h with appropriate antibodies: either the anti-caveolin-1 antibody or the anti-MGST1 antibody (EPR 7934). The grid was washed in PBS 0.1% BSAc, and incubated with appropriate secondary antibodies coupled to gold nanoparticles (1:20 dilution in PBS 0.1% BSAc): either the anti-mouse antibody coupled to 6 nm gold nano-particles to visualize the caveolin-1β alone or the anti-rabbit antibody coupled to 6 nm gold nano-particles to visualize the MGST1 alone. Then, the grid was washed with several solutions: PBS 0.1% BSAc, PBS buffer, PBS 2.5% (v:v) glutaraldehyde, PBS buffer, H_2O. Negative staining was performed with NanoVan before TEM imaging.

2.6.4. TEM observations

Grids were examined under a JEM 1400 TEM operating at 120 kV (JEOL). TEM Images were acquired using a post-column high-resolution (9 megapixels) high-speed camera (RIO9; Gatan), and processed with Digital Micrograph (Gatan) and ImageJ (open source software, Research Services Branch, National Institutes of Mental Health, Bethesda, MD).

2.7. GST activity

GST catalyzes the conjugation of 1-chloro-2,4-dinitrobenzene (CDNB) with reduced glutathione (GSH), and produces a dinitrophenyl thioether (GS-DNB) which possesses a high extinction coefficient at 340 nm ($\varepsilon_{340\ nm} = 9.6\ mM^{-1}\ cm^{-1}$) that promotes its detection by spectrophotometry. The rate of increase in the absorbance at 340 nm is directly proportional to the GST activity in the sample. Activities were determined according to Habig et al. [33] in 100 mM potassium phosphate, pH 6.5, containing 0.1 mM ethylenediaminetetraacetic acid, 0.1% (v:v) Triton X-100 in the presence of 5 mM GSH and 1 mM CDNB. The sample and reaction buffer volumes were adjusted to a final volume of 200 μL to accommodate a 96-well microplate format. The absorbance at 340 nm was monitored with a microplate spectrophotometer (Epoch, BioTek) every minute for 15 min. The rate of the spontaneous conjugation was determined under the same conditions, and subtracted from that of the wells containing the sample. All samples were assayed in triplicate at 30 °C.

3. Results

3.1. Formation of intracellular vesicles in Sf21 insect cells expressing canine caveolin-1β

According to Li et al. [9], the heterologous expression in *Sf21* insect cells of the isoform β of canine caveolin-1 (caveolin-1β) using a baculovirus-based vector led to the formation of intracellular vesicles of diameter similar to those of *caveolae* and enriched in caveolin-1β. Such vesicles may serve as membrane reservoirs and promote the production of a functional MP. To test this hypothesis, a plasmid co-expressing both caveolin-1β and hMGST1 proteins (Fig. S1) was designed and used for the preparation of the baculovirus. After cell infection and protein expression, the evaluation of membrane morphology modifications, including the presence of intracellular vesicles, in the *Sf21* insect cells was performed by transmission electron microscopy (TEM). First, considering the cytoplasm of *Sf21* insect cells transfected by the only caveolin-1β-coding baculovirus at four days post-infection, numerous vesicles were observed (Fig. 2A) in agreement with Li et al. [9]. In contrast, no apparent caveolae (like invaginations) or caveolar structures (like rosettes) at the plasma membrane could be observed in *Sf21* insect cells transfected only by the hMGST1-coding baculovirus (Fig. 2C). We sometimes noticed, for some cells, the destruction of the nuclear membrane, as already reported for baculovirus infections [39], and the presence of vesicles within the nucleus (Fig. S3A).

When the *Sf21* insect cells were infected with a baculovirus carrying the co-expression vector for caveolin-1β and hMGST1, TEM also revealed the presence of numerous vesicles in the cytosol of the infected insect cells (Fig. 2B). Thus, TEM observations showed that the infection of *Sf21* insect cells by a baculovirus coding for the expression of caveolin-1β, either in the absence or in the presence of hMGST1, induced the formation of numerous cytoplasmic vesicles.

3.2. Characterization of caveolin-1β and hMGST1 enriched membranes

The protein production was characterized from cell pellets obtained after centrifugation of *Sf21* cell cultures stopped at five days post-infection. Each pellet contained about 2.10^8 insect cells.

The procedure used to collect the membrane fractions is described in Fig. 1.The TM fraction contained about 5.8 to 8.6 mg of total proteins.

The co-expression of both caveolin-1β and hMGST1 was followed by Western blots, using either a histidine probe for His-tagged caveolin-1β

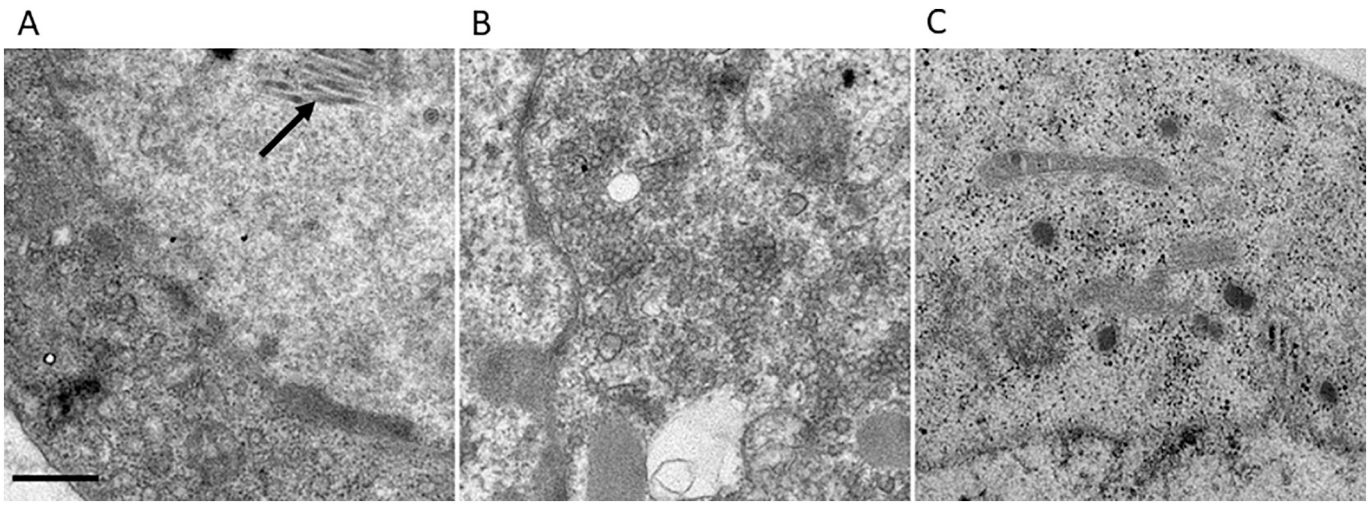

Fig. 2. Visualization by transmission electron microscopy of membrane vesicles induced in insect cells (*Sf21*) when infected by a baculovirus. Observation at four days post-infection. A, membranes vesicles in the cytoplasm of an insect cell induced by the expression of canine caveolin-1β only. Arrow shows baculovirus particles in the nucleus. B, membranes vesicles in the cytoplasm of an insect cell induced by the co-expression of canine caveolin-1β and hMGST1. C, cytoplasm of an insect cell induced by the expression of hMGST1 only. Scale bar 500 nm.

or an anti-MGST1 antibody (Abcam, EPR 7934) for hMGST1. The expression of both proteins was detectable in lysis extracts (see Fig. 3A1, lane L) as well as in the P2 and TM fractions (Fig. 3A1). The apparent molecular weights of caveolin-1β and hMGST1 observed on the Western blots are consistent with the protein sequences, suggesting that extensive proteolysis did not occur during preparation. In the F1 sucrose fraction, caveolin-1β was detectable, but not hMGST1 (Fig. 3A1). The F1 fraction located at the meniscus of the centrifuge tube corresponds to a less dense medium as measured by refractometry (1.391 value of refractive index), attributable to a higher lipid/protein ratio. Alternatively, the denser F6 to F8 fractions were enriched in both caveolin-1β and hMGST1 (Fig. 3A1), and GST activity measurement of the membrane fractions indicated the presence of hMGST1 in the F5 to F10 samples (Fig. 3A2).

Using TEM and immuno-detection with an anti-caveolin antibody coupled to gold nano-particles, the presence of caveolin-1β in the F7 fraction was observed (Fig. 4A and E). Moreover, the presence of MGST1 on the vesicles or at least on membranous structures was also evidenced by TEM in the presence of the anti-MGST1 (Abcam, EPR 7934) antibodies coupled to gold nano-particles (Fig. 4C and E). Thus it is possible to detect MGST1 and this detection is more marked in vesicles and in membrane structures.

3.3. GST activity in the presence or absence of caveolin-1β

The GST activity of all membrane fractions isolated from the co-expression of caveolin-1β and hMGST1 was measured (Fig. S4A). Two activity areas were clearly separated according to their position in the sucrose density gradient (Fig. 3A2): the first one, corresponding to fractions F1 to F3 was located in the lighter density zone, and the second one, fractions F6 to F9, was localized at about 44% (w:w) sucrose (n = 1.405–1.413), percentage defined in the presence of 10% (v:v) glycerol. The maximal activity of 0.05 μmol min^{-1} (total protein $mg)^{-1}$ at 30 °C (Fig. 3A2) was observed for the F7 fraction, and this is relatively high, as it compares well to the activity of 0.015–0.030 μmol min^{-1} (total protein $mg)^{-1}$ that was measured for recombinant rat enzyme in the total membranes of COS cells [15].

In order to evaluate the influence of caveolin-1β on the hMGST1 expression, hMGST1 was expressed in the absence of caveolin-1β. For that, the same plasmid without the caveolin-1β gene was used under similar experimental conditions, and the absence of expression of caveolin-1β was checked (see Fig. S5A). In order to increase the resolution of both the protein concentration and GST activity curves, more fractions of smaller volumes were collected from the centrifugation tubes at the end of the isopycnic run. The presence of the hMGST1 protein was estimated along the steps of the preparation (Fig. 3B1) by Western blots revealed by an anti-MGST1 antibody (Abcam, EPR 7934). The hMGST1 is clearly detected in the lysis extract and TM fractions, and slightly in the P2 fraction (Fig. 3B1). The hMGST1 was not detectable in the F2 fraction (n = 1.382), but it was visible slightly in F12 (n = 1.402) and mainly in F13 (n = 1.405) membrane fractions (Fig. 3B1). The measurement of GST activity (Fig. 3B2) showed a marked peak for membranes of even lighter densities (n < 1.387) than observed in Fig. 3A2. For these membranes of intermediate densities (F5-F14, n = 1.389–1.406), the activity for F13 of 0.012 μmol min^{-1} (total protein $mg)^{-1}$ at 30 °C (Fig. 3B2) was much reduced compared to the experiment where hMGST1 was co-expressed with caveolin-1β (compare Figs. S4B and S4A). These experiments thus evidenced an influence of the presence of caveolin-1β and the generated membrane vesicles on the distribution of hMGST1 in the dense sucrose membrane fractions, as well as on the GST activity measured.

In order to evaluate the possible contribution of the insect endogenous MGSTs on the measured GST activity, caveolin-1β was expressed in the absence of hMGST1. Under that condition, caveolin-1β was found in the light (F2) and intermediate (F9-F12) density fractions (Fig. S5B). The presence of the endogenous insect MGSTs was evaluated along the steps of the preparation by Western blots revealed by an anti-MGST1 antibody (Abcam, EPR 7934). A band corresponding to the expected apparent MW of MGSTs was detected in the lysis extract, in the P2 fraction and in the TM fraction (Fig. 3C1). This cross-reacting protein, the endogenous MGST, was not detectable in the F1 sucrose fraction, but it was present in the F12 to F14 membrane fractions (Fig. 3C1). In addition, a major band was also observed at about 37 kDa, which may correspond to a trimer of the insect MGST. Nevertheless, it is noteworthy that in the Western blot analysis of the membranes containing caveolin-1β and hMGST1 (see Fig. 3A1, F6-8 fractions), or hMGST1 alone (Fig. 3B1, F12-13 fractions), this constitutive trimer form of MGST1 was not visible, even when 20 μg was loaded (Fig. S6A). In terms of enzymatic activity, the measure of GST activity showed a peak for the F12-F15 fractions (n = 1.405–1.413), with the F13 fraction giving an activity of 0.026 μmol min^{-1} (total protein $mg)^{-1}$ at 30 °C (Fig. 3C2). This activity is higher than that of hMGST1 expressed in the absence of caveolin-1β (Fig. 3B2), but in which endogenous MGST was also not detectable by Western blot (Fig. 3B1).

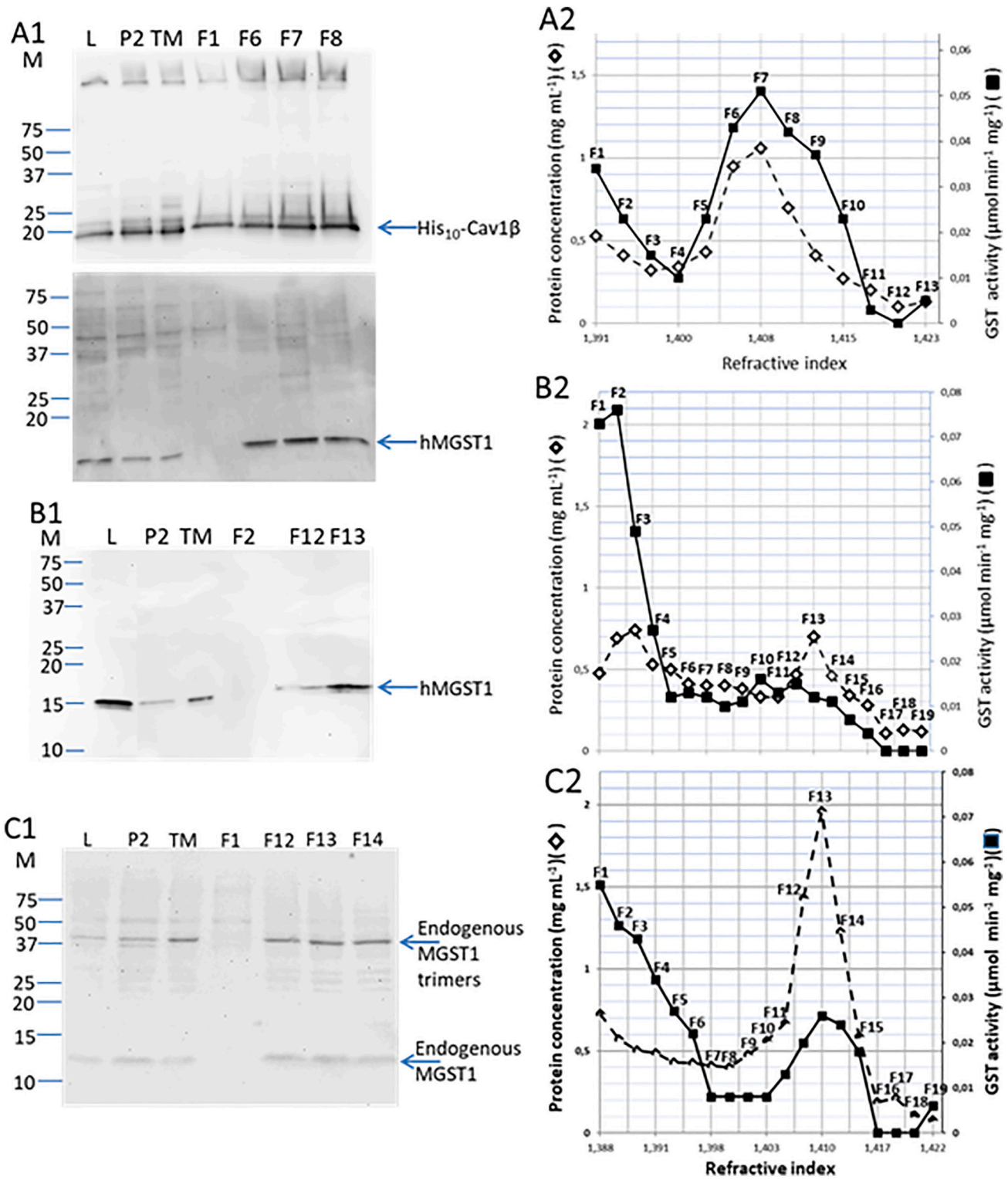

Fig. 3. Characterization of membranes after expression of caveolin-1β and hMGST1 (A1 and A2); hMGST1 alone (B1 and B2) and caveolin-1β alone (C1 and C2). Various samples along the preparation were analyzed: L, lysis extract; P2, insoluble fraction; TM, total membranes; F1-19, fractions (1 mL for the co-expression samples; 0.5 mL for the single-expression samples) collected at the termination of the isopycnic centrifugation run, the fractions are numbered from the top of the centrifugation tube. A1, B1 and C1, analyses by Western blots. For each sample, the equivalent of 5 µg of total proteins was analyzed to determine its content either in His-tag caveolin-1β, revealed by a His probe (A1), or in hMGST1, revealed by an anti-MGST1 antibody (Abcam, EPR 7934) (A1, B1 and C1). M, molecular mass markers positions are indicated (in kDa). A2, B2 and C2, determination of total protein concentration and GST activity (basal activity is the activity in the absence of NEM activation). For each collected fraction from the isopycnic sucrose gradient, the total protein concentration (◇, dashed line) and GST activity (■, continuous line) are plotted as a function of the refractive index of the corresponding fraction. The data plotted are representative of two to three independent experiments with similar results.

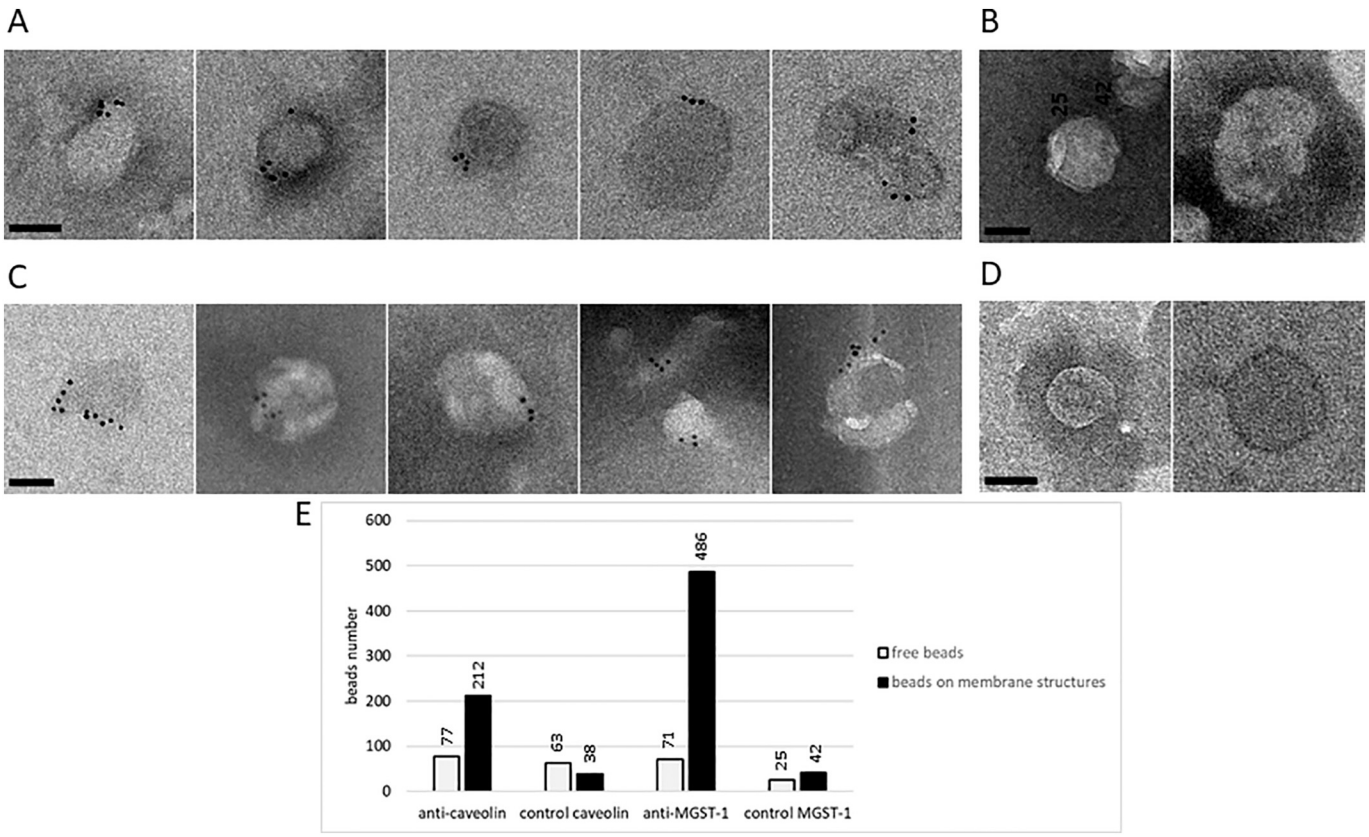

Fig. 4. Visualization by transmission electron microscopy and immuno-detection of membrane vesicles in the cytoplasm of insect cells (*Sf21*) at four days post-infection. Membrane vesicles were induced in *Sf21* cells when infected by a baculovirus for the co-expression of caveolin-1β and hMGST1. A, visualization of caveolin-1β on membrane vesicles corresponding to the membrane F7 fraction (see Fig. 3A1). Caveolin-1β was immuno-detected with a mouse anti-caveolin antibody and an anti-mouse secondary antibody coupled to a 6 nm diameter gold nano-particle. B, control visualization on similar membrane vesicles as in A but replacing anti-caveolin antibody with BSA. C, visualization of hMGST1 on similar membrane vesicles as in A. MGST1 was immuno-detected with a rabbit anti-MGST1 antibody and an anti-rabbit secondary antibody coupled to a 6 nm diameter gold nano-particle. D, control visualization on similar membrane vesicles as in C but replacing anti-MGST1 antibody with BSA. Scale bars 50 nm. E, histogram representing the number of nano-particles (beads) numbered on membrane structures and outside membrane structures (free) in 50 fields (1.69 μm^2 each field) for all the observations A, B, C and D. (For interpretation of the references to colour in this ffgure legend, the reader is referred to the web version of this article.)

In order to be able to discriminate between the insect MGSTs and the cloned hMGST1, a more specific antibody was used, the monoclonal antibody anti-MGST1 EPR 7935 (Abcam) that is directed against a C-terminal region of the mammalian MGST1. Analysis by Western blot confirmed the absence of cross-reaction with the insect MGSTs (Fig. S6B), in contrast to the detection observed with the antibody EPR 7934 (Fig. 3C1).

3.4. Quantification of hMGST1 production

The production of hMGST1 was quantified along the preparation by measuring the amount of hMGST1 in lysis extract, total membrane fractions, and sucrose membrane fractions by Western blots revealed with the anti-MGST1 antibody (Abcam, EPR 7935), which recognizes the human and rat MGST1 but does not cross-react with the insect endogenous MGSTs. Quantitative evaluation was made by comparison with rat microsomes [36] (Fig. 5), in which MGST1 represents about 3% of total proteins [28]. The ratio of hMGST1 per μg of total proteins was higher in the singly-expressed hMGST1 as compared to the co-expressed hMGST1 for lysis extract (Fig. 5A), whereas for the total membranes (TM) this ratio was similar for both expression conditions (Fig. 5B). However, it was higher in the co-expressed hMGST1-enriched membrane sucrose fractions as compared to the singly-expressed ones (Fig. 5C). These data were used to estimate the isolation yields (Table I). The co-expression with caveolin-1β induced a four-fold increased amount of hMGST1 in the most enriched membrane fraction (6.1 μg instead of 1.5 μg without caveolin-1β). Moreover, in this Table are presented the GST activities relative either to the total protein (GST activity) or to the estimated hMGST1 amount (specific GST activity). The co-expression of hMGST1 with caveolin-1β yielded a GST specific activity in the most enriched fraction that was largely increased, from 5.2 to 8.4 μmol min^{-1} (hMGST1 mg)$^{-1}$ (Table I), consistent with, and even higher than, the activity of 4.4 μmol min^{-1} (hMGST1 mg)$^{-1}$ measured by Weinander et al. in the COS cells system [15].

Memb. fraction, membrane fraction corresponds to 1 mL volume of the most hMGST1-enriched membrane fraction, corresponding to densities of $n = 1.404–1.407–1.407$ for the three co-expression experiments and $n = 1.400–1.405$ for the two single expression experiments.

3.5. Caveolin-1β and hMGST1 detected in insect cells by TEM

Two separate sets of immunodetection were performed to detect the presence of caveolin-1β and hMGST1 within insect cells. As a matter of fact, when using two different secondary antibodies, goat anti-mouse IgG1 for anti-caveolin antibody, and goat anti-rabbit IgG for anti-MGST1 antibody (EPR 7935, ABCAM), the immunodetection of hMGST1 failed, probably due to the use of goat anti-rabbit IgG. Consequently, the anti-MGST1 antibody (MA5-34942), which is specific of hMGST1 and produced in mouse, was used.

Immuno-detection of these two heterologous MPs revealed that they

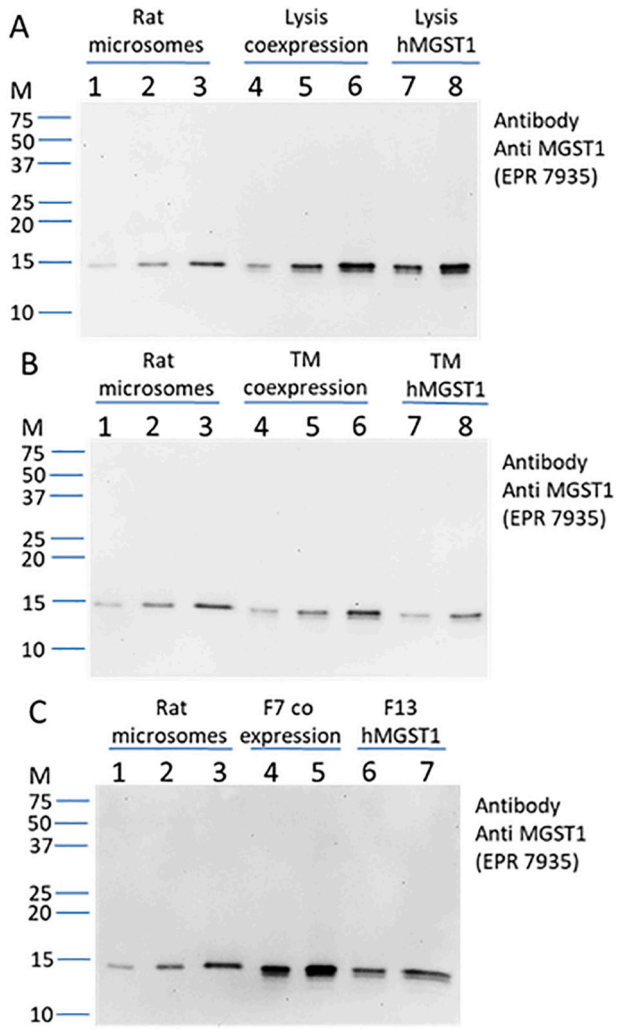

Fig. 5. Quantification of MGST1 in membranes from caveolin-1β and hMGST1 co-expression and hMGST1 single-expression samples. Various samples were analyzed to determine their content in hMGST1 by Western blots revealed by an anti-MGST1 antibody (Abcam, EPR 7935) which does not cross-react with insect endogenous MGSTs. Lysis, lysis extract; TM, total membranes; F, fractions from the sucrose gradient; they were compared to a range of rat microsomes, which contain 3% of MGST1; lanes 1 to 3: 0.05, 0.1 and 0.2 μg of proteins. M: molecular mass markers are indicated (in kDa). A, analysis of Lysis samples: lanes 4 and 7: 1.25 μg of proteins; lanes 5 and 8: 2.5 μg of proteins; lane 6: 5 μg of proteins were analyzed. B, analysis of TM samples: lanes 4 to 8: as in A. C, analysis of F samples: lanes 4 and 5: 1.3 and 2.6 μg of proteins of F7 caveolin-1β and hMGST1 co-expression fraction were analyzed; lanes 6 and 7: 1.7 and 3.4 μg of proteins of F13 hMGST1 expression fraction were analyzed.

were expressed on cytoplasmic vesicles (Figs. 6 and S3). They were also present on mitochondria and plasma membranes (Fig. 6D) and also in nuclear vesicles and viral particles (Fig. S3). Nevertheless, on the cytoplasmic vesicles, the number of beads was considerably higher for caveolin-1β detection than for hMGST1 detection. It appeared that hMGST1 was not totally present in caveolin-1β-induced vesicles but that a proportion of this MP was localized free in the cytoplasm (Fig. 6D), probably in unfolded form.

4. Discussion

4.1. *Sf21 insect cells as a convenient heterologous expression system*

The *Sf21* insect cells is a widely used heterologous expression system that presents some advantages, including the various opportunities relying on baculovirus transfection technology [40]. In particular, for expressing MPs, it compares well with *E. coli* due to the fact that it is much easier to lyse the cells in order to obtain a membrane fractionation including internal vesicles. Regarding caveolin-1 expression, *Sf21* cells have otherwise the advantage of not expressing endogenous caveolin isoforms [9].

Here, we have evaluated the benefit of using the co-expression of hMGST1 with caveolin-1β in *Sf21* insect cells to express functional hMGST1. The production process includes the transfection of *Sf21* insect cells with a shuttle vector pKL in order to obtain the first generation of recombinant baculovirus (V0). Then, a baculovirus stock was constituted by amplification and, finally, a large volume of cell culture was infected with the recombinant baculovirus. The gene of interest is cloned into the shuttle vector pKL, which controls the expression of the target gene by either the strong *Autographa californica* multiple nuclear polyhedrosis virus (AcMNPV) polyhedrin (polH) or the p10 promoters. This can be further adapted for the expression of multi-gene complexes using the Multibac system, as reviewed in [41]. Accordingly, the plasmid pKL allows the direct expression of two proteins. Indeed, this system offers two main advantages. First, the iterative addition of nucleotide sequences on the same vector is facilitated, allowing the constitution of large complex of proteins step by step; thus, *hmgst1* gene has been inserted together with *cav-1β* gene. Second, the presence of YFP protein reporter in the baculovirus genome gives a valuated tool for the production monitoring. Using this system, a large amount of caveolin-1β (Fig. 3A1) was produced for the formation of intracellular vesicles. Indeed, it was essential to obtain such a high level of expression of caveolin-1β as it has been shown that the presence of intracellular vesicles is highly dependent on the expression level of caveolin-1 [9]. These vesicles could be visualized in the insect cells after 4 days of cultures post-infection. Moreover, caveolin-1β was associated to these vesicles, as its presence was evidenced by immunodetection using gold nanoparticles (Fig. 6A). We chose to express caveolin-1β, the shorter isoform, because it has been demonstrated that after recombinant expression in *Sf21* insect cells, both caveolins α and β can independently generate these intracellular vesicles, and thus caveolin-1 residues 1–31

Table I
Influence of the co-expression of caveolin-1β on the production of active hMGST1 in enriched membrane fractions.

Samples	Co-expression Cav 1 B/hMGST1				Expression hMGST1			
	Protein amount (mg)	hMGST1 amount (μg)	GS transferase activity (μmol min^{-1} protein mg^{-1})	GS transferase activity (μmol min^{-1} hMGST1 mg^{-1})	Protein amount (mg)	hMGST1 amount (μg)	GS transferase activity (μmol min^{-1} protein mg^{-1})	GS transferase activity (μmol min^{-1} hMGST1 mg^{-1})
TM	7.25±1.4[a]	15.2±3.46[b]	0.033±0.0015	16.8±1.8	5.5–3.64[a]	10.7-7.2[b]	0.035-0.035	18-17.5
Memb. fraction	1.21±0.13[a]	6.13±1.4[b]	0.042±0.008	8.4±1.3	0.7–0.54[a]	1.46-1.86[b]	0.012-0.016	5.75-4.64

[a] Data determined by Bradford assay. Data represent three independent experiments for the caveolin-1β and hMGST1 co-expression and two independent experiments for the single expression of hMGST1.

[b] Data determined from quantiffcation of hMGST1 band on the Western blot relatively to a range of rat microsomes containing 3% of MGST1 (as in Fig. 5) using Quantity One (Biorad) with non-saturating loadings.

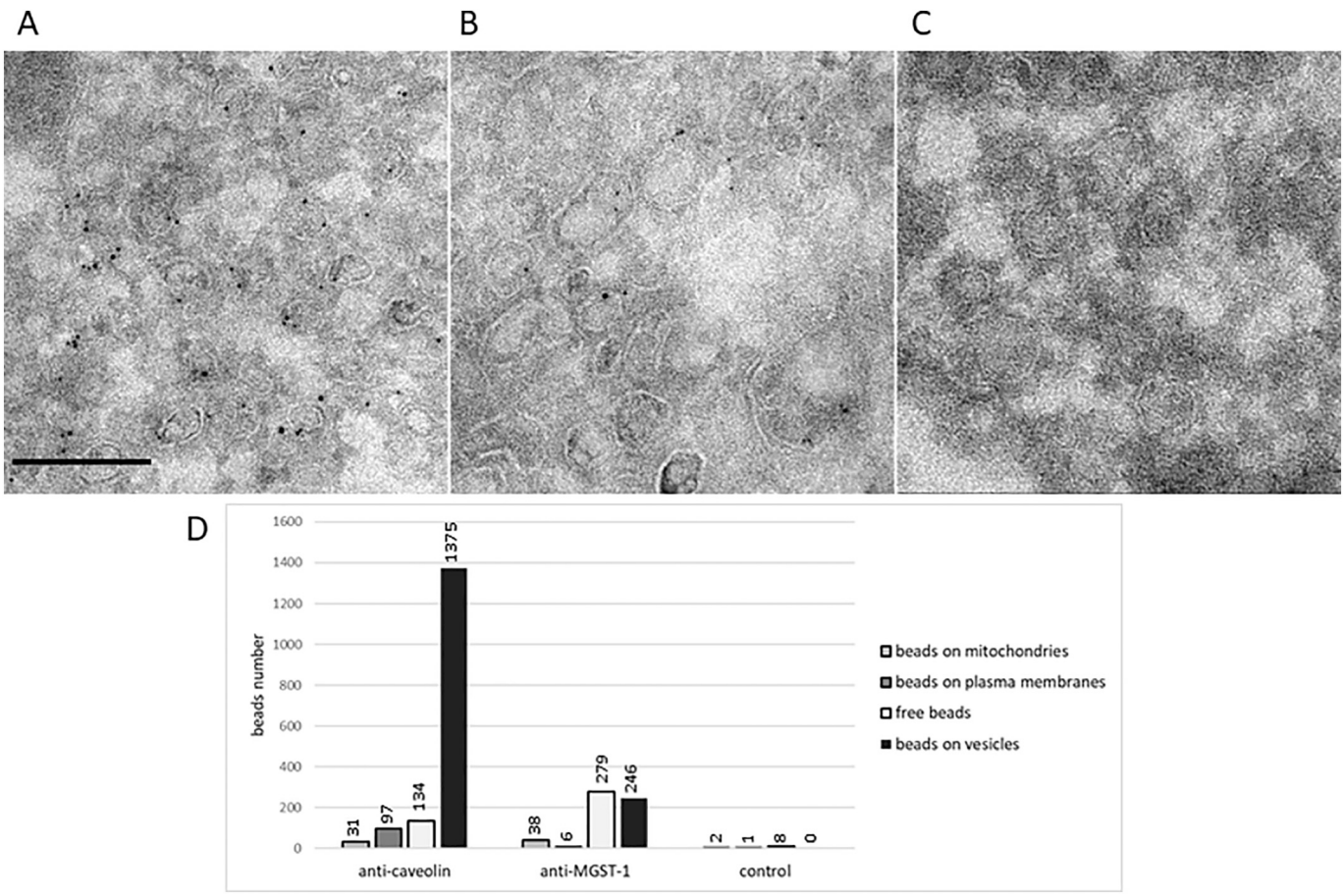

Fig. 6. Visualization by transmission electron microscopy of membrane vesicles induced in insect cells (*Sf21*) by the co-expression of caveolin-1β and hMGST1. Observation at four days post-infection. A, visualization by immuno-detection of caveolin-1β with a mouse anti-caveolin antibody and an anti-mouse secondary antibody coupled to a 6 nm diameter gold nano-particle. B, visualization by immuno-detection of hMGST1 with a mouse anti-MGST1 antibody (MA5–34942) and an anti-mouse secondary antibody coupled to a 6 nm diameter gold nano-particle. C, control visualization on similar insect cells as in A and B but replacing primary antibody with BSA. Scale bar 200 nm. D, histogram representing the number of nano-particles (beads) numbered on mitochondria, plasma membranes, outside the membrane structures (free) and on vesicles in 50 fields (10 cells and 5 fields (2.56 μm^2 each field) per cell) for all the observations A, B and C. (For interpretation of the references to colour in this ffgure legend, the reader is referred to the web version of this article.)

are not required for their formation [9].

4.2. Caveolin-1β induced vesicles

We observed numerous cytoplasmic vesicles when caveolin-1β was overexpressed in *Sf21* cells using a different construct and shuttle vector for the production of recombinant baculovirus and infection of *Sf21* cells than Li et al. [9]. Our TEM observations including immunolabeling showed that caveolin-1β is associated with these internal vesicles, thereby evidencing the vesiculating efficiency of caveolin-1β. As a matter of fact, caveolin-1 has been demonstrated to exhibit a strong membrane membrane-curving activity linked to its oligomerization [9,12,42], and hence can induce local remodeling of the ER membrane where it is biosynthesized, or of membranes from its downward intracellular trafficking, ultimately leading to membrane fission and vesicle formation. This behavior, still present in spite of a local membrane lipid composition different in *Sf21* insect and mammalian cells, well illustrates the powerful driving force for membrane curving that is displayed by caveolin-1.

In addition, these vesicles present a remarkable homogenous distribution of size which correlates with its specific intrinsic membrane-curving [43]. However, membrane fractionation experiments on density gradient showed that these caveolin-1β-containing vesicles displayed a rather large density range, meaning a defined range of protein-to-lipid ratios, which indicates a diverse protein environment accompanying the vesiculation step, possibly corresponding to different functional sub-domains of the ER [44], and/or to membranes from intracellular trafficking. ER remodeling induced by MP overexpression, as observed for only few specific MPs, has been considered as a manifestation of either a "membrane proliferation" secondary to a cell stress (e.g. the unfolded protein response, but there are also various other cellular mechanisms) leading to membrane lipid synthesis activation, or of a specific "geometrical response" due to a strong membrane-curving property of the overexpressed MP [45], although the two aspects are not necessarily exclusive. The case of caveolin-1β heterologous overexpression may be representative of the second phenomenon, but there remains the question of an additional "reservoir effect" that could accommodate some other MPs. The co-expression of hMGST1will provide some clues about this question.

4.3. Influence of caveolin-1β on hMGST1 expression: localization and quantification

As indicated by Weinander et al., [15], it may be difficult to estimate the amount of MGST1 from different species using a rabbit anti-rat enzyme serum. We chose to quantify hMGST1, relatively to rat MGST1, using antibodies described as recognizing both rat and human MGST1: the antibodies EPR 7934 and 7935 (Abcam). We have observed different sensitivities between these two antibodies for the human enzyme recognition, in favor of the second one. Moreover, it was

important to use this second antibody for quantification, because, as we verified, and in contrast to the first one, it does not cross-react with the insect endogenous MGSTs.

Regarding the expression level of hMGST1 in the absence and in the presence of caveolin-1β, we observe a higher amount of hMGST1 in the lysis extract for singly-expressed hMGST1 (Fig. 5A). Consequently, the caveolin-1β co-expression did not increase the hMGST1 expression per se, and has even the reverse effect. In addition, the preparation of total membranes reveals similar amounts of hMGST1 when hMGST1 is singly expressed or co-expressed with caveolin-1β (Fig. 5B). Therefore, even if hMGST1 is expressed at high level when expressed alone, the protein is not stored only in the membrane fraction, probably due to partial misfolding.

hMGST1 expression alone did not induce the formation of vesicles within *Sf21* cells (Fig. 2C). Its co-expression with caveolin-1β did not impede the formation of the cytosolic vesicles enriched in caveolin-1β and fractions of expressed hMGST1 are located in these vesicles (Fig. 6B and D). So hMGST1 partially follows "passively" the efficient membrane-curving driving force exhibited by caveolin-1β.

This is line with results from membrane fractionation using isopycnic centrifugation. The heterologous singly-expressed hMGST1 is distributed sparsely on several fractions (F5 to F14, $n = 1.389–1.406$, Fig. 3B2), whereas when co-expressed with caveolin-1β, its distribution is narrowed within few fractions (F6-F9, $n = 1.405–1.412$, Fig. 3A2). This demonstrates the membrane density shifting effect of its co-expression with caveolin-1β. In addition, the amount of hMGST1 in the most active membrane fraction (F7) corresponds to 40% of the amount of hMGST1 in total membranes in the case of co-expression, whereas it represents only a small amount (18% in F13) in the case of singly-expressed hMGST1 (Fig. 5C, Table I). This suggests that the presence of caveolin-1β and the induced vesicles found in the membrane fractions is able to concentrate hMGST1 in this density range (around $n = 1.41$). It can thus be inferred that caveolin-1β is able to divert and sequester hMGST1, considered as a cargo, to the neoformed ectopic intracellular vesicles. In addition, a sub-population of caveolin-1β-containing vesicles has a lower density (thus a lower protein-to-lipid ratio) and are devoid of such heterologous MP cargo. This last characteristics suggests that these "light" vesicles are formed either from a membrane domain less prone to heterologous MP integration (e.g. different lipid composition or curvature), or result from a delayed vesiculization process within downward intracellular membrane trafficking. Therefore, these vesicles represent a distinct vesicle population with a different intracellular fate.

The expression of caveolin-1β in the absence of hMGST1 in *Sf21* cells has revealed the presence of an endogenous MGST activity, attributed to seven homologous isoforms of insect MGSTs (Jonathan Landry, EMBL, personal communication). These endogenous MGSTs can be distinguished from the mammalian ones using Western blots that show the stability of their trimer association. Interestingly, they are detected in membrane fractions of the same density range as the heterologous hMGST1. However, they are not detected in both singly-expressed and co-expressed hMGST1 in *Sf21* cells, suggesting a kind of retro-control exerted by the heterologous expressed protein on the endogenous expression level involving these enzymes.

Regarding the lowest density membrane fractions, the presence of a notable GST activity raises the question of the possible presence of another population of *Sf21* GSTs (Fig. 3A2-B2-C2). These proteins could adsorb on light membranes with $n \leq 1.387$ and $n \leq 1.396$ in the absence and presence of caveolin-1β, respectively, whatever the presence or absence of hMGST1 expression. This evidences that caveolin-1β-induced vesicles of low density may also contain proteins that are diverted from their normal intracellular fate, constituting a cargo of endogenous proteins associated with the caveolin-1β-containing membranes.

4.4. Influence of caveolin-1β on hMGST1 specific activity

When co-expressed or not with caveolin-1β in *Sf21* cells, the GST activity was measured in membrane fractions enriched in hMGST1 (Fig. 3A2 and B2). Thanks to the hMGST1 amount specific quantification, we could calculate the corresponding specific enzymatic activities. We have first to mention that we did not observe any stimulation by N-ethylmaleimide (NEM). This is in agreement with the reported observations of NEM activation of the purified human enzyme, but not of the enzyme in microsomes, at least for the human isoform (in contrast to the rat one) [46].The evaluated hMGST1 specific activity in the respective most active fractions (see Table I) are 5.2 μmol.min^{-1}.hMGST1 mg^{-1} in the absence of caveolin-1β and 8.4 μmol.min^{-1}.hMGST1 mg^{-1} in the presence of caveolin-1β (at 30 °C). These values are higher than that described in previous studies (in all cases for CDNB substrate and without NEM activation): 1.88 μmol min^{-1} purified native hMGST1 mg^{-1} (at 37 °C) [47], 1.9 μmol min^{-1} purified native hMGST1 mg^{-1} (at 30 °C) [46], and 4.4 μmol min^{-1} partially purified *E coli*-expressed hMGST1 mg^{-1} (at 30 °C) [15]. Therefore, the significantly higher specific enzymatic activity of hMGST1 in the co-expression system, than in the single expression one, reinforces the view that some fraction of this MP is addressed into the ectopic heterologous intracellular vesicles. It may be considered that even if endogenous MGST is present at a low concentration, its specific activity may be higher and contribute to the global activity. The more favorable membrane environment may be in connection to specific relationships with caveolin-1β and/or the lipid environment locally segregated and/or to the high local curvature.

4.5. Perspectives in the general context of heterologous MP expression

While the co-expression of caveolin-1 with associated soluble proteins in insect cells has been reported [9], the production of a MP devoid of functional link with caveolin-1 has not yet been described. In caveolin-1-expressing mammalian cells, *caveolae* membranes have been described to be formed with a specific lipid composition (constituting membrane microdomains), accompanied by protein segregation leading to an enrichment of certain ones [7] and exclusion of many others [48]. However, in *Sf21* cells, there is neither endogenous caveolin-1 homologues nor *caveolae* membrane structures. The heterologous expressed caveolin-1β does not follow the same intracellular trafficking to the plasma membrane as in mammalian cells and essentially remains in internal membrane compartments under the form of neoformed intracellular vesicles (Figs. 6A and S3A). These vesicles enriched in caveolin-1β will thus possess different molecular characteristics to that of *caveolae*, in particular regarding the local segregation of MPs. In addition, in the *Sf21* heterologous expression system, the membrane lipid composition is clearly different. It is thus difficult to a priori predict the co-localization relationships between caveolin-1β and another MP simultaneously co-expressed in such heterologous system.

Here, we have evidenced that heterologous expressed hMGST1 is in part directed to intracellular vesicles as the consequence of its co-expression with caveolin-1β in *Sf21* cells. These intracellular vesicles enriched in caveolin-1β can thus be envisioned as playing the role of "intracellular carriers", able of handling some cargo MPs. This observation may have important implications in the general context of heterologous expression of MPs, due to this unique addressing characteristics in well-defined membrane compartments. In particular, in the perspective of improving heterologous MP production, this could be valuable in terms of convenient handling, isolation and functional preservation. It remains to explore and determine whether this method could be applied to various types of MPs, regarding typically their organelle origin, size, number of transmembrane segments, dependence on the lipid environment, including nature and curvature. Also, various expression hosts (e.g. prokaryotes, yeasts, pluricellular low eukaryotes such as parasites and insects) will also have to be tested and compared.

5. Conclusion

When co-expressed with hMGST1 in *Sf21* insect cells, caveolin-1β, a

membrane-curving MP, retains its capacity to induce intracellular vesicles in the host. In addition, hMGST1 is partially addressed to these intracellular vesicles. Thus, caveolin-1β is able to induce a shift of the membrane harboring hMGST1 (and also possibly endogenous homologue isoforms) likely thanks to a passive trapping mechanism into the neoformed ectopic vesicles enriched in caveolin-1β. Noteworthy, the co-expressed hMGST1 exhibits an increased specific enzymatic activity, witnessing its new membrane environment. The contribution of an additional "reservoir effect", due to an increased membrane phase available to the co-expressed MP, remains to be investigated, as well as the possible application of such a situation to other types of MPs, including those from plasma membrane.

CRediT authorship contribution statement

CJ and MG conceived and designed experimental work; NP, DD, AR, CG, CJ and MG performed experiments; CJ, MG, NJ and SO wrote the paper; all authors contributed to the manuscript.

Declaration of competing interest

The authors declare that they have no known competing interests or personal relationships that could have appeared to influence the work reported in this paper.

Acknowledgements

We thank Pascal Drevet, Virginie Ropars and Audrey Coens for baculovirus preparation and insect cultures (platform Proteins expression in insect cells of I2BC supported by French Infrastructure for Integrated Structural Biology (FRISBI) ANR-10-INBS-05-05), Claire Boulogne for her help in MET experiments (platform Imagerie-Gif core facility supported by l'Agence Nationale de la Recherche (ANR-11-EQPX-0029/Morphoscope, ANR-10-INBS-04/FranceBioImaging, ANR-11-IDEX-0003-02/Saclay Plant Sciences), Alexandre Pozza for the conditions of insect cells lysis, Cédric Montigny for the quantification of Western blots and all of them for fruitful discussions. We thank Jonathan Landry for kindly providing the *Sf*21 MGST amino acid sequences. This work was supported by the French National Research Agency under Grant n° ANR-17-CE11-015-01 and by the French Infrastructure for Integrated Structural Biology (FRISBI) ANR-10-INBS-05.

Appendix A. Supplementary data

Supplementary data to this article can be found online at https://doi.org/10.1016/j.bbamem.2022.183922.

References

[1] J.P. Overington, B. Al-Lazikani, A.L. Hopkins, How many drug targets are there? Nat. Rev. Drug Discov. 5 (2006) 993–996, https://doi.org/10.1038/nrd2199.
[2] A.G. Lee, How lipids affect the activities of integral membrane proteins, Biochim. Biophys. Acta BBA - Biomembr. 1666 (2004) 62–87, https://doi.org/10.1016/j.bbamem.2004.05.012.
[3] A. Kesidis, P. Depping, A. Lodé, A. Vaitsopoulou, R.M. Bill, A.D. Goddard, A. J. Rothnie, Expression of eukaryotic membrane proteins in eukaryotic and prokaryotic hosts, Methods 180 (2020) 3–18, https://doi.org/10.1016/j.ymeth.2020.06.006.
[4] J.A. Lyons, A. Shahsavar, P.A. Paulsen, B.P. Pedersen, P. Nissen, Expression strategies for structural studies of eukaryotic membrane proteins, Curr. Opin. Struct. Biol. 38 (2016) 137–144, https://doi.org/10.1016/j.sbi.2016.06.011.
[5] R. Assenberg, P.T. Wan, S. Geisse, L.M. Mayr, Advances in recombinant protein expression for use in pharmaceutical research, Curr. Opin. Struct. Biol. 23 (2013) 393–402, https://doi.org/10.1016/j.sbi.2013.03.008.
[6] S. Monier, R.G. Parton, F. Vogel, J. Behlke, A. Henske, T.V. Kurzchalia, VIP21-caveolin, a membrane protein constituent of the caveolar coat, oligomerizes in vivo and in vitro, Mol. Biol. Cell 6 (1995) 911–927, https://doi.org/10.1091/mbc.6.7.911.
[7] W. Jung, E. Sierecki, M. Bastiani, A. O'Carroll, K. Alexandrov, J. Rae, W. Johnston, D.J.B. Hunter, C. Ferguson, Y. Gambin, N. Ariotti, R.G. Parton, Cell-free formation and interactome analysis of caveolae, J. Cell Biol. 217 (2018) 2141–2165, https://doi.org/10.1083/jcb.201707004.
[8] R.G. Parton, K.-A. McMahon, Y. Wu, Caveolae: formation, dynamics, and function, Curr. Opin. Cell Biol. 65 (2020) 8–16, https://doi.org/10.1016/j.ceb.2020.02.001.
[9] S. Li, K.S. Song, S.S. Koh, A. Kikuchi, M.P. Lisanti, Baculovirus-based expression of mammalian caveolin in Sf21 insect cells: a model system for the biochemical and morphological study of Caveolae biogenesis, J. Biol. Chem. 271 (1996) 28647–28654, https://doi.org/10.1074/jbc.271.45.28647.
[10] K.S. Song, S. Li, T. Okamoto, L.A. Quilliam, M. Sargiacomo, M.P. Lisanti, Co-purification and direct interaction of Ras with caveolin, an integral membrane protein of caveolae microdomains: detergent-free purification of Caveolae membranes, J. Biol. Chem. 271 (1996) 9690–9697, https://doi.org/10.1074/jbc.271.16.9690.
[11] K.S. Song, P.E. Scherer, Z. Tang, T. Okamoto, S. Li, M. Chafel, C. Chu, D.S. Kohtz, M.P. Lisanti, Expression of Caveolin-3 in skeletal, cardiac, and smooth muscle cells: Caveolin-3 is a component of the sarcolemma and co-fractionates with dystrophin and dystrophin-associated glycoproteins, J. Biol. Chem. 271 (1996) 15160–15165, https://doi.org/10.1074/jbc.271.25.15160.
[12] P.J. Walser, N. Ariotti, M. Howes, C. Ferguson, R. Webb, D. Schwudke, N. Leneva, K.-J. Cho, L. Cooper, J. Rae, M. Floetenmeyer, V.M.J. Oorschot, U. Skoglund, K. Simons, J.F. Hancock, R.G. Parton, Constitutive formation of caveolae in a bacterium, Cell 150 (2012) 752–763, https://doi.org/10.1016/j.cell.2012.06.042.
[13] J. Shin, Y.-H. Jung, D.-H. Cho, M. Park, K.E. Lee, Y. Yang, C. Jeong, B.H. Sung, J.-H. Sohn, J.-B. Park, D.-H. Kweon, Display of membrane proteins on the heterologous caveolae carved by caveolin-1 in the Escherichia coli cytoplasm, Enzym. Microb. Technol. 79–80 (2015) 55–62, https://doi.org/10.1016/j.enzmictec.2015.06.018.
[14] R. Morgenstern, J. Zhang, K. Johansson, Microsomal glutathione transferase 1: mechanism and functional roles, Drug Metab. Rev. 43 (2011) 300–306.
[15] R. Weinander, E. Mosialou, J. DeJong, C.P.D. Tu, J. Dypbukt, T. Bergman, H. J. Barnes, J.O. Höög, R. Morgenstern, Heterologous expression of rat liver microsomal glutathione transferase in simian COS cells and Escherichia coli, Biochem. J. 311 (1995) 861–866, https://doi.org/10.1042/bj3110861.
[16] S. Bakari, M. Lembrouk, L. Sourd, F. Ousalem, F. André, S. Orlowski, M. Delaforge, A. Frelet-Barrand, Lactococcus lactis is an efficient expression system for mammalian membrane proteins involved in liver detoxification, CYP3A4, and MGST1, Mol. Biotechnol. 58 (2016) 299–310, https://doi.org/10.1007/s12033-016-9928-z.
[17] W.R. Pearson, Phylogenies of glutathione transferase families, in: Methods Enzymol, Elsevier, 2005, pp. 186–204. https://linkinghub.elsevier.com/retrieve/pii/S0076687905010128.
[18] H. Shi, L. Pei, S. Gu, S. Zhu, Y. Wang, Y. Zhang, B. Li, Glutathione S-transferase (GST) genes in the red flour beetle, Tribolium castaneum, and comparative analysis with five additional insects, Genomics 100 (2012) 327–335, https://doi.org/10.1016/j.ygeno.2012.07.010.
[19] P.-J. Jakobsson, R. Morgenstern, J. Mancini, A. Ford-Hutchinson, B. Persson, Common structural features of mapeg-a widespread superfamily of membrane associated proteins with highly divergent functions in eicosanoid and glutathione metabolism, Protein Sci. 8 (1999) 689–692, https://doi.org/10.1110/ps.8.3.689.
[20] P.J. Holm, P. Bhakat, C. Jegerschöld, N. Gyobu, K. Mitsuoka, Y. Fujiyoshi, R. Morgenstern, H. Hebert, Structural basis for detoxification and oxidative stress protection in membranes, J. Mol. Biol. 360 (2006) 934–945, https://doi.org/10.1016/j.jmb.2006.05.056.
[21] T.D. Boyer, D.A. Vessey, E. Kempner, Radiation inactivation of microsomal glutathione S-transferase, J. Biol. Chem. 261 (1986) 16963–16968.
[22] R. Morgenstern, J.W. DePIERRE, H. Jörnvall, Microsomal glutathione transferase. Primary structure, J. Biol. Chem. 260 (1985) 13976–13983.
[23] P.L. Pettersson, S. Thorén, P. Jakobsson, Human microsomal prostaglandin E synthase 1: a member of the MAPEG protein superfamily, in: Methods Enzymol, Elsevier, 2005, pp. 147–161. https://linkinghub.elsevier.com/retrieve/pii/S0076687905010098.
[24] W.B. Jakoby, The glutathione S -transferases: a group of multifunctional detoxification proteins, in: A. Meister (Ed.), Adv. Enzymol. - Relat. Areas Mol. Biol, John Wiley & Sons, Inc., Hoboken, NJ, USA, 1978, pp. 383–414, https://doi.org/10.1002/9780470122914.ch6.
[25] C. Frova, Glutathione transferases in the genomics era: new insights and perspectives, Biomol. Eng. 23 (2006) 149–169, https://doi.org/10.1016/j.bioeng.2006.05.020.
[26] R.C. Fahey, A.R. Sundquist, Evolution of glutathione metabolism, in: A. Meister (Ed.), Adv. Enzymol. - Relat. Areas Mol. Biol, John Wiley & Sons, Inc, Hoboken, NJ, USA, 1991, pp. 1–53, https://doi.org/10.1002/9780470123102.ch1.
[27] J. Coleman, M. Blake-Kalff, E. Davies, Detoxification of xenobiotics by plants: chemical modification and vacuolar compartmentation, Trends Plant Sci. 2 (1997) 144–151, https://doi.org/10.1016/S1360-1385(97)01019-4.
[28] R. Morgenstern, C. Guthenberg, J. Depierre, Microsomal glutathione S-transferasePurification, initial characterization and demonstration that it is not identical to the cytosolic glutathione S-transferases A, B and C, Eur J Biochem. 128 (1982) 243–248.
[29] M. Shimoji, R.A. Figueroa, E. Neve, D. Maksel, G. Imreh, R. Morgenstern, E. Hallberg, Molecular basis for the dual subcellular distribution of microsomal glutathione transferase 1, Biochim. Biophys. Acta BBA - Biomembr. 2017 (1859) 238–244, https://doi.org/10.1016/j.bbamem.2016.11.014.
[30] M.E. Horbach, H. Sies, T.P.M. Akerboom, Identification of a hepatic plasma membrane glutathione S-transferase activated by N-ethylmaleimide, Biochim. Biophys. Acta BBA - Biomembr. 1148 (1993) 61–66, https://doi.org/10.1016/0005-2736(93)90160-2.

[31] M. Islinger, G.H. Lüers, H. Zischka, M. Ueffing, A. Völkl, Insights into the membrane proteome of rat liver peroxisomes: microsomal glutathione-S-transferase is shared by both subcellular compartments, Proteomics 6 (2006) 804–816, https://doi.org/10.1002/pmic.200401347.
[32] A. Siritantikorn, K. Johansson, K. Åhlen, R. Rinaldi, T. Suthiphongchai, P. Wilairat, R. Morgenstern, Protection of cells from oxidative stress by microsomal glutathione transferase 1, Biochem. Biophys. Res. Commun. 355 (2007) 592–596, https://doi.org/10.1016/j.bbrc.2007.02.018.
[33] Pabst Habig, Glutathione S.-transferases Jakoby, The first enzymatic step in mercapturic acid formation, J. Biol. Chem. 249 (1974) 7130–7139.
[34] D. Sari, K. Gupta, D.B.T.G. Raj, A. Aubert, P. Drncová, F. Garzoni, D. Fitzgerald, I. Berger, The MultiBac baculovirus/insect cell expression vector system for producing complex protein biologics, in: M.C. Vega (Ed.), Adv. Technol. Protein Complex Prod. Charact, Springer International Publishing, Cham, 2016, pp. 199–215, https://doi.org/10.1007/978-3-319-27216-0_13.
[35] A.R. Bernard, M. Lusti-Narasimhan, K.M. Radford, R.S. Hale, E. Sebille, P. Graber, Downstream processing of insect cell cultures, Cytotechnology 20 (1996) 239–257, https://doi.org/10.1007/BF00350404.
[36] M. Delaforge, D. Servent, P. Wirsta, C. Ducrocq, D. Mansuy, M. Lenfant, Particular ability of cytochrome P-450 CYP3A to reduce glyceryl trinitrate in rat liver microsomes: subsequent formation of nitric oxide, Chem. Biol. Interact. 86 (1993) 103–117, https://doi.org/10.1016/0009-2797(93)90115-F.
[37] P.E. Scherer, Z. Tang, M. Chun, M. Sargiacomo, H.F. Lodish, M.P. Lisanti, Caveolin isoforms differ in their N-terminal protein sequence and subcellular distribution. Identification and epitope mapping of an isoform-specific monoclonal antibody probe, J. Biol. Chem. 270 (1995) 16395–16401, https://doi.org/10.1074/jbc.270.27.16395.
[38] P.E. Scherer, T. Okamoto, M. Chun, I. Nishimoto, H.F. Lodish, M.P. Lisanti, Identification, sequence, and expression of caveolin-2 defines a caveolin gene family, Proc. Natl. Acad. Sci. 93 (1996) 131–135, https://doi.org/10.1073/pnas.93.1.131.
[39] X. Zhang, K. Xu, D. Wei, W. Wu, K. Yang, M. Yuan, Baculovirus infection induces disruption of the nuclear lamina, Sci. Rep. 7 (2017), https://doi.org/10.1038/s41598-017-08437-5.
[40] M.M. van Oers, G.P. Pijlman, J.M. Vlak, Thirty years of baculovirus–insect cell protein expression: from dark horse to mainstream technology, J. Gen. Virol. 96 (2015) 6–23, https://doi.org/10.1099/vir.0.067108-0.
[41] C. Bieniossek, T. Imasaki, Y. Takagi, I. Berger, MultiBac: expanding the research toolbox for multiprotein complexes, Trends Biochem. Sci. 37 (2012) 49–57, https://doi.org/10.1016/j.tibs.2011.10.005.
[42] N. Ariotti, J. Rae, N. Leneva, C. Ferguson, D. Loo, S. Okano, M.M. Hill, P. Walser, B. M. Collins, R.G. Parton, Molecular characterization of caveolin-induced membrane curvature, J. Biol. Chem. 290 (2015) 24875–24890, https://doi.org/10.1074/jbc.M115.644336.
[43] N. Jamin, M. Garrigos, C. Jaxel, A. Frelet-Barrand, S. Orlowski, Ectopic neo-formed intracellular membranes in Escherichia coli: a response to membrane protein-induced stress involving membrane curvature and domains, Biomolecules 8 (2018) 88, https://doi.org/10.3390/biom8030088.
[44] E.M. Lynes, T. Simmen, Urban planning of the endoplasmic reticulum (ER): how diverse mechanisms segregate the many functions of the ER, Biochim. Biophys. Acta BBA - Mol. Cell Res. 1813 (2011) 1893–1905, https://doi.org/10.1016/j.bbamcr.2011.06.011.
[45] J. Royes, V. Biou, N. Dautin, C. Tribet, B. Miroux, Inducible intracellular membranes: molecular aspects and emerging applications, Microb. Cell Factories 19 (2020), https://doi.org/10.1186/s12934-020-01433-x.
[46] E. Mosialou, C. Andersson, G. Lundqvist, G. Andersson, T. Bergman, H. Jörnvall, R. Morgenstern, Human liver microsomal glutathione transferase: substrate specificity and important protein sites, FEBS Lett. 315 (1993) 77–80, https://doi.org/10.1016/0014-5793(93)81137-O.
[47] L.I. McLellan, C.R. Wolf, J.D. Hayes, Human microsomal glutathione S-transferase. Its involvement in the conjugation of hexachlorobuta-1,3-diene with glutathione, Biochem. J. 258 (1989) 87–93, https://doi.org/10.1042/bj2580087.
[48] E. Shvets, V. Bitsikas, G. Howard, C.G. Hansen, B.J. Nichols, Dynamic caveolae exclude bulk membrane proteins and are required for sorting of excess glycosphingolipids, Nat. Commun. 6 (2015), https://doi.org/10.1038/ncomms7867.